An Improved Peak Voltage Calculation Method for Compensation Components in S-S and LCC-S Compensated Wireless Power Transfer Systems

Yu, G.; Ye, P.; Grazian, F.; Dong, J.; Soeiro, Thiago B.; Bauer, P.

DOI
10.23919/EPE23ECCEEurope58414.2023.10264576

Publication date
2023

Document Version
Accepted author manuscript

Published in
Proceedings of the 25th European Conference on Power Electronics and Applications

An Improved Peak Voltage Calculation Method for Compensation Components in S-S and LCC-S Compensated Wireless Power Transfer Systems

Guangyao Yu[1], Pengcheng Ye[1], Francesca Grazian[1], Jianning Dong[1], Thiago Batista Soeiro[2], and Pavol Bauer[1]

[1]EEMCS, Delft University of Technology, Delft, The Netherlands
[2]EEMCS, University of Twente, Enschede, The Netherlands

***Abstract*—The pursuit of battery charging technology for electric vehicle (EV) has led to extensive research on the inductive-based wireless power transfer (WPT) systems. In this paper, the compensation component (including coils) stresses will be studied in two commonly adopted compensation topologies, namely S-S and LCC-S compensations. Due to the peak voltage calculation inaccuracy for certain components based on conventional fundamental frequency analysis, an improved peak voltage calculation method is introduced in closed form, which is proved to be more accurate by both simulation and experiments.**

***Index Terms*—Wireless Power Transmission, Compensation, Resonant Converter, Closed form equations.**

I. Introduction

Compensation network plays an indispensable role in wireless power transfer (WPT) systems, which is used to improve power transfer efficiency. Due to the resonance characteristics, the compensation components may be subject to high voltage and current stresses, which needs to be considered throughout the system design. Series-series (S-S) and LCC-S compensation topologies featuring constant current (CC) and constant voltage (CV) output at resonant operating frequency are two widely used compensations since the component values are independent of the coupling and load conditions [1], [2].

In [3], [4], the compensation component stresses were studied between S-S and LCC-LCC compensations at 7.7 kW and 20 kW, respectively. A comprehensive comparison of four resonant topologies, i.e., S-S, S-LCC, LCC-S and LCC-LCC, was studied in terms of efficiency and component stresses in [5]. A comparative study focusing on efficiency and circuit parameter sensitivity between S-S and LCC-S compensations was given in [2]. However, few literature has been found to provide accurate peak voltage calculation methods for the compensation components. Peak voltage directly affects the insulation reliability of the circuit system, which could be even worse in a higher frequency operation condition [6], [7], therefore, to determine it accurately is the first step to design a system with reliable electrical insulation.

In this paper, the voltage and current stresses of the compensation components (including coils) of S-S and LCC-S topologies will be studied at 3 kW power level, which is the WPT1 power level suggested by SAE J2954 for wireless power charging of light-duty electric vehicles [8]. The study of current stress is meaningful and necessary since its value under fundamental frequency analysis directly affects the accuracy of peak voltage calculation, which will be seen in Section II. The rest of this paper is arranged as follows: Firstly, voltage and current stresses of compensation components will be given based on fundamental frequency analysis, which is also referred to as first harmonic approximation (FHA) method. Secondly, the inaccuracy of certain components' peak voltage calculation will be pointed out through a specific example. The improved formulas will be derived afterwards, which is then verified through simulation. Finally, experiments were carried out to validate the improved method through a laboratory WPT setup.

This project has received funding from the Electronic Components and Systems for European Leadership Joint Undertaking under grant agreement No 876868. This Joint Undertaking receives support from the European Union's Horizon 2020 research and innovation programme and Germany, Slovakia, Netherlands, Spain, Italy.

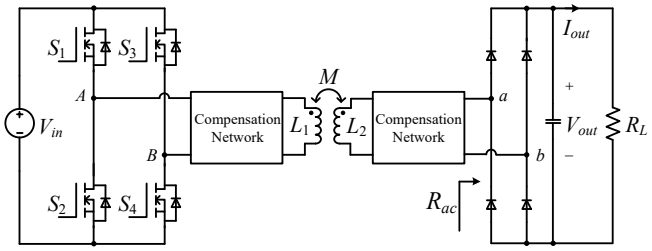

Fig. 1: Schematic of a WPT system.

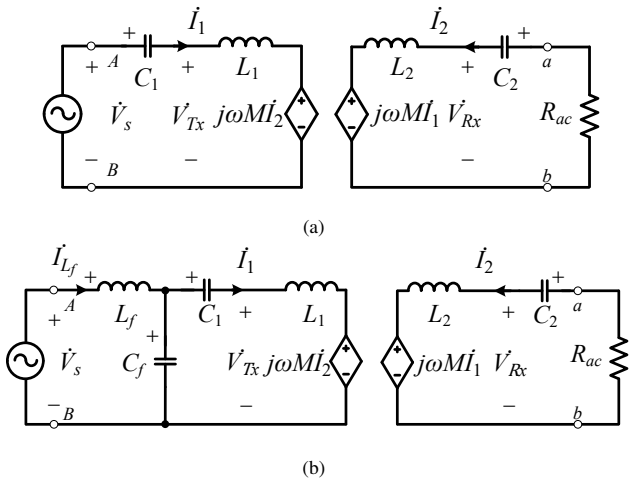

Fig. 2: Equivalent circuits of S-S and LCC-S compensations based on the transformer's mutual inductance model. (a) S-S. (b) LCC-S.

II. S-S and LCC-S Compensations

Fig. 1 shows a typical schematic of the WPT system. The H-bridge inverter composed of switches S_1-S_4 operates close to the resonant frequency to produce a high-frequency AC voltage to excite the primary side coil while the passive full-wave diode rectifier is used for the secondary side rectification. R_L is the equivalent load resistance modeling the power of subsequent stage, which is defined as $R_L = \frac{V_{out}}{I_{out}}$. The compensation networks of S-S and LCC-S topologies are illustrated in Fig. 2 with defined current and voltage reference direction. The loosely coupled transformer is modeled through a mutual inductance model [9]. To facilitate the analysis, the lump resistance modeling the losses of the WPT system is not included.

In Fig. 2, $\dot{V}_s$, $\dot{I}_1$, $\dot{I}_2$, $\dot{I}_{L_f}$, $\dot{V}_{Tx}$ and $\dot{V}_{Rx}$ are corresponding phasors. R_{ac} is the equivalent resistance seen before the rectification stage (cf. Fig. 1) with a value of $R_{ac} = \frac{8}{\pi^2}R_L$ [10]. Herein, the amplitude of $\dot{V}_s$ is assumed as the root-mean-square (rms) value of the fundamental frequency component of the inverter output voltage. So, when the inverter operates at natural resonant frequency with a square wave output voltage, the amplitude of $\dot{V}_s$ is: $V_s = |\dot{V}_s| = \frac{2\sqrt{2}}{\pi}V_{in}$.

A. Component Stress based on First Harmonic Approximation Method (FHA)

1) S-S Compensation : Based on Kirchhoff's voltage law, the equations for Fig. 2(a) can be written as

$$\begin{cases} \dot{V}_s = (j\omega L_1 + \frac{1}{j\omega C_1})\dot{I}_1 + j\omega M\dot{I}_2, \\ j\omega M\dot{I}_1 + (j\omega L_2 + \frac{1}{j\omega C_2} + R_{ac})\dot{I}_2 = 0. \end{cases} \tag{1}$$

In (1), ω is the angular frequency, M is the mutual inductance. At resonant frequency of ω_0, the capacitor values of C_1 and C_2 are selected as

$$C_1 = \frac{1}{\omega_0^2 L_1}, C_2 = \frac{1}{\omega_0^2 L_2}. \tag{2}$$

Based on (1) and (2), the voltage and current stresses of each component can be derived. The general and simplified expressions of peak voltage and current rms values are given in Table I and II, respectively. In Table II, R_{ac} can also be expressed as $R_{ac} = P_o\frac{\omega_0^2 M^2}{V_s^2}$ with P_o being the processed power.

TABLE I: General expressions of compensation component stress in the S-S topology.

	C_1	C_2	Primary Coil	Secondary Coil
RMS Current	$\lvert\dot{I}_1\rvert$	$\lvert\dot{I}_2\rvert$	$\lvert\dot{I}_1\rvert$	$\lvert\dot{I}_2\rvert$
Peak Voltage	$\sqrt{2}\lvert\frac{\dot{I}_1}{j\omega_0 C_1}\rvert$	$\sqrt{2}\lvert\frac{\dot{I}_2}{j\omega_0 C_2}\rvert$	$\sqrt{2}\lvert j\omega_0 L_1\dot{I}_1 + j\omega_0 M\dot{I}_2\rvert$	$\sqrt{2}\lvert j\omega_0 M\dot{I}_1 + j\omega_0 L_2\dot{I}_2\rvert$

TABLE II: Simplified expressions of compensation component stress in the S-S topology with $R_{ac} = P_o\frac{\omega_0^2 M^2}{V_s^2}$.

	C_1	C_2	Primary Coil	Secondary Coil
RMS Current	$\frac{P_o}{V_s}$	$\frac{V_s}{\omega_0 M}$	$\frac{P_o}{V_s}$	$\frac{V_s}{\omega_0 M}$
Peak Voltage	$\frac{\sqrt{2}\omega_0 L_1 P_o}{V_s}$	$\frac{\sqrt{2}L_2 V_s}{M}$	$\sqrt{2}V_s\sqrt{1+(\frac{L_1 R_{ac}}{\omega_0 M^2})^2}$	$\sqrt{2}V_s\sqrt{(\frac{L_2}{M})^2+(\frac{R_{ac}}{\omega_0 M})^2}$

2) LCC-S Compensation : Based on Kirchhoff's voltage law, the equations for Fig. 2(b) can be written as

$$\begin{cases} \dot{V}_s = j\omega L_f\dot{I}_{L_f} + \frac{1}{j\omega C_f}(\dot{I}_{L_f} - \dot{I}_1), \\ \dot{V}_s = j\omega L_f\dot{I}_{L_f} + (j\omega L_1 + \frac{1}{j\omega C_1})\dot{I}_1 + j\omega M\dot{I}_2, \\ j\omega M\dot{I}_1 + (j\omega L_2 + \frac{1}{j\omega C_2} + R_{ac})\dot{I}_2 = 0. \end{cases} \tag{3}$$

At resonant frequency of ω_0, the capacitor values of C_f, C_1 and C_2 are selected as

$$C_f = \frac{1}{\omega_0^2 L_f}, C_1 = \frac{1}{\omega_0^2(L_1 - L_f)}, C_2 = \frac{1}{\omega_0^2 L_2}. \tag{4}$$

TABLE III: General expressions of compensation component stress in the LCC-S topology.

	C_1	C_2	C_f	Primary Coil	Secondary Coil	L_f
RMS Current	$\lvert\dot{I}_1\rvert$	$\lvert\dot{I}_2\rvert$	$\lvert\dot{I}_{L_f}-\dot{I}_1\rvert$	$\lvert\dot{I}_1\rvert$	$\lvert\dot{I}_2\rvert$	$\lvert\dot{I}_{L_f}\rvert$
Peak Voltage	$\sqrt{2}\lvert\frac{\dot{I}_1}{j\omega_0 C_1}\rvert$	$\sqrt{2}\lvert\frac{\dot{I}_2}{j\omega_0 C_2}\rvert$	$\sqrt{2}\lvert\frac{1}{j\omega_0 C_f}(\dot{I}_{L_f}-\dot{I}_1)\rvert$	$\sqrt{2}\lvert j\omega_0 L_1\dot{I}_1+j\omega_0 M\dot{I}_2\rvert$	$\sqrt{2}\lvert j\omega_0 L_2\dot{I}_2+j\omega_0 M\dot{I}_1\rvert$	$\sqrt{2}\lvert j\omega_0 L_f\dot{I}_{L_f}\rvert$

TABLE IV: Simplified expressions of compensation component stress in the LCC-S topology with $R_{ac}=\frac{1}{P_o}(\frac{M}{L_f}V_s)^2$.

	C_1	C_2	C_f	Primary Coil	Secondary Coil	L_f
RMS Current	$\frac{V_s}{\omega_0 L_f}$	$\frac{MV_s}{L_f R_{ac}}$	$\sqrt{(\frac{P_o}{V_s})^2+(\frac{V_s}{\omega_0 L_f})^2}$	$\frac{V_s}{\omega_0 L_f}$	$\frac{MV_s}{L_f R_{ac}}$	$\frac{P_o}{V_s}$
Peak Voltage	$\sqrt{2}(\frac{L_1}{L_f}-1)V_s$	$\sqrt{2}\omega_0 L_2\frac{MV_s}{L_f R_{ac}}$	$\sqrt{2}\omega_0 L_f\sqrt{(\frac{P_o}{V_s})^2+(\frac{V_s}{\omega_0 L_f})^2}$	$\sqrt{2}V_s\sqrt{(\frac{L_1}{L_f})^2+(\frac{\omega_0 M^2}{L_f R_{ac}})^2}$	$\sqrt{2}V_s\sqrt{(\frac{M}{L_f})^2+(\frac{\omega_0 L_2 M}{L_f R_{ac}})^2}$	$\sqrt{2}\frac{\omega_0 L_f P_o}{V_s}$

Based on (3) and (4), the current of $\dot{I}_1$ and $\dot{I}_2$ can be derived as

$$\dot{I}_1=\frac{\dot{V}_s}{j\omega_0 L_f}, \dot{I}_2=-\frac{1}{R_{ac}}\frac{M}{L_f}\dot{V}_s. \tag{5}$$

So, according to (3), (4) and (5), the voltage and current stresses of each component can be derived. The general and simplified expressions are given in Table III and IV. In Table IV, R_{ac} can also be expressed as $R_{ac}=\frac{1}{P_o}(\frac{M}{L_f}V_s)^2$.

III. Inaccuracy of Derived Formulas

Simulation results from circuit simulator PLECS based on a specific example are adopted to verify the calculations. Voltage and current sources are applied as the load for S-S and LCC-S compensations, respectively.

The coil parameters are taken from the laboratory prototype designed at 3 kW power rating with $L_1=338$ μH and $L_2=226$ μH. The operating frequency f_0 is 85 kHz recommended by SAE J2954 standard [8]. V_{in} (see Fig. 1) is selected as 400 V.

A. S-S Compensation

The simulated and calculated results for each component are summarized in Table V with $M=90$ μH and $P_o=3$ kW. The relative error is defined by $\varepsilon=\frac{\text{Calculated Value}-\text{Simulated Value}}{\text{Simulated Value}}$. For PLECS solver, the max step size is 1e-8 s and the relative tolerance is 1e-4.

As it can be seen from Table V, the calculated peak voltage for both primary and secondary coils is not as accurate as other values. Besides, both of the calculated values are smaller than the simulated ones. However, the current calculation based on FHA method has high accuracy.

TABLE V: Compensation component stress in S-S topology with $M=$ 90 μH, $P_o=3$ kW.

	C_1	C_2	Primary Coil	Secondary Coil
Cal.[1] RMS Current (A)	8.33	7.49	8.33	7.49
Sim.[2] RMS Current (A)	8.34	7.51	8.34	7.51
Error of ε (%)	-0.12	-0.27	-0.12	-0.27
Cal. Peak Voltage (V)	2126.7	1278.9	2186.8	1398.7
Sim. Peak Voltage (V)	2125.1	1275.4	2520.8	1720.1
Error of ε (%)	0.08	0.27	-13.25	-18.68

[1,2] Cal. and Sim. are short for Calculated and Simulated in this paper.

B. LCC-S Compensation

The simulated and calculated results for each component are summarized in Table VI with $M=90$ μH, $P_o=3$ kW, $L_f=100$ μH.

TABLE VI: Compensation component stress in LCC-S topology with $M=$ 90 μH, $P_o=3$ kW, $L_f=$ 100 μH.

	C_1	C_2	C_f	Primary Coil	Secondary Coil	L_f
Cal. RMS Current (A)	6.74	9.26	10.72	6.74	9.26	8.33
Sim. RMS Current (A)	6.74	9.30	10.35	6.74	9.30	8.41
Error of ε (%)	0	-0.43	3.57	0	-0.43	-0.95
Cal. Peak Voltage (V)	1212.1	1580.0	809.5	1832.8	1645.1	629.2
Sim. Peak Voltage (V)	1220.2	1580.0	756.0	1800.8	1940.0	1029.2
Error of ε (%)	-0.66	0	7.08	1.78	-15.2	-38.9

As it can be seen from Table VI, the calculated peak voltage for the secondary coil and L_f is not accurate, similar to S-S compensation, both of the calculated values are smaller than the simulated ones.

C. Improved Method

Due to the high accuracy of the current calculation based on FHA method, the more accurate component peak voltage can then simply be calculated based on Kirchhoff's voltage law considering the voltage across the related compensation capacitors.

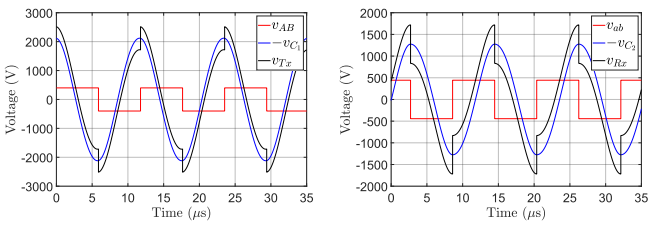

(a) (b)

Fig. 3: Simulated waveforms of the S-S compensation, defined reference direction is shown in Fig. 2. (a) Primary side. (b) Secondary side.

1) S-S Compensation : Fig. 3 shows the simulated waveforms at 3 kW, which is used to help explain the following calculation.

Refer to Fig. 1 and Fig. 2, the voltage across the primary side coil can be expressed as: $v_{Tx} = v_{AB} - v_{C_1}$. Since $\dot{I}_1$ and $\dot{V}_s$ are in phase, so, the voltage of $-v_{C_1}$ is 90° (or $\frac{\pi}{2}$ radian) ahead of v_{AB} (cf. Fig. 3(a)). Therefore, the peak voltage is

$$\hat{V}_{Tx\_improved} = V_{in} + \hat{V}_{C_1} = V_{in} + \frac{\pi\omega_0 L_1 P_o}{2V_{in}}. \quad (6)$$

Similarly, the peak voltage across the secondary coil is

$$\hat{V}_{Rx\_improved} = V_{out} + \hat{V}_{C_2} = \frac{\pi^2\omega_0 M P_o}{8V_{in}} + \frac{4L_2 V_{in}}{\pi M}. \quad (7)$$

2) LCC-S Compensation: Fig. 4 shows the simulated waveforms at 3 kW and 300 W, which is used to help explain the following calculation. The voltage across L_f can be expressed as

$$v_{L_f} = v_{AB} - v_{C_f}. \quad (8)$$

The phasor representation of v_{C_f} is

$$\dot{V}_{C_f} = (\frac{1}{j\omega_0 C_1} + j\omega_0 L_1)\dot{I}_1 + j\omega_0 M\dot{I}_2 = (j\omega_0 L_f + Z_r)\dot{I}_1. \quad (9)$$

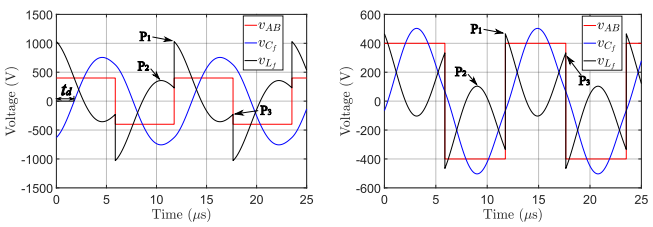

(a) (b)

Fig. 4: Simulated waveforms of the LCC-S compensation, defined reference direction is shown in Fig. 2. (a) $P_o = 3$ kW. (b) $P_o = 300$ W.

In (9), $Z_r = \frac{\omega_0^2 M^2}{R_{ac}}$. Substitute $\dot{I}_1$ from (5) into (9), then

$$\dot{V}_{C_f} = (j\omega_0 L_f + Z_r)\dot{I}_1 = \dot{V}_s - jZ_r\frac{\dot{V}_s}{\omega_0 L_f}. \quad (10)$$

Assuming $\dot{V}_s = V_s\angle 0°$, at the instant when v_{AB} changes from $-V_{in}$ to V_{in}, the instantaneous value of v_{C_f} is the imaginary part of (10) multiplied by $\sqrt{2}$, i.e., $-\sqrt{2}\frac{\omega_0 M^2 V_s}{L_f R_{ac}}$. Therefore, the voltage across L_f at point P_1 is

$$\hat{V}_{L_f\_improved} = V_{in} + \sqrt{2}\frac{\omega_0 M^2 V_s}{L_f R_{ac}} = V_{in} + \frac{\pi\omega_0 L_f P_o}{2V_{in}}. \quad (11)$$

However, by further checking Fig. 4, there are another two local peaks of P_2 and P_3. The proof that the voltage at P_1 is the global peak is given in Appendix A.

For the peak voltage across the secondary coil, it is similar to S-S compensation, which is

$$\hat{V}_{Rx\_improved} = V_{out} + \hat{V}_{C_2} = \frac{M}{L_f}V_{in} + \frac{\pi}{2}\frac{\omega_0 L_2 L_f P_o}{MV_{in}}. \quad (12)$$

The improved formulas are summarized in Table VII.

TABLE VII: Improved formulas for peak voltage calculation.

S-S	$\hat{V}_{Tx} = V_{in} + \frac{\pi\omega_0 L_1 P_o}{2V_{in}}$	$\hat{V}_{Rx} = \frac{\pi^2\omega_0 M P_o}{8V_{in}} + \frac{4L_2 V_{in}}{\pi M}$
LCC-S	$\hat{V}_{L_f} = V_{in} + \frac{\pi\omega_0 L_f P_o}{2V_{in}}$	$\hat{V}_{Rx} = \frac{MV_{in}}{L_f} + \frac{\pi\omega_0 L_2 L_f P_o}{2MV_{in}}$

D. Discussion on Improved Formulas

For both methods based on FHA and improved formulas, a minimum peak voltage for primary and secondary coils in S-S compensation, and for L_f and secondary coil in LCC-S compensation can be derived. Since $a + b \geq 2\sqrt{ab}$ when $a \geq 0$ and $b \geq 0$, therefore, the minimum peak voltage values for the components derived from Table II, Table IV and Table VII are given as follows.

1) S-S Compensation:

According to the FHA method given in Table II:

$$\hat{V}_{Tx} \geq 2\sqrt{\omega_0 L_1 P_o},\ \hat{V}_{Rx} \geq 2\sqrt{\omega_0 L_2 P_o}. \quad (13)$$

According to the improved method:

$$\hat{V}_{Tx} \geq \sqrt{2\pi\omega_0 L_1 P_o},\ \hat{V}_{Rx} \geq \sqrt{2\pi\omega_0 L_2 P_o}. \quad (14)$$

2) LCC-S Compensation:

According to the FHA method given in Table IV:

For L_f, a similar formula of the minimum peak voltage cannot be derived. For L_2, it is:

$$\hat{V}_{Rx} \geq 2\sqrt{\omega_0 L_2 P_o}. \tag{15}$$

According to the improved method:

$$\hat{V}_{L_f} \geq \sqrt{2\pi\omega_0 L_f P_o},\ \hat{V}_{Rx} \geq \sqrt{2\pi\omega_0 L_2 P_o}. \tag{16}$$

From (14) and (16), it can be found that the minimum peak voltage expressions have the same form.

IV. Simulation Verification

The newly derived formulas will be verified by simulation at different mutual inductance, power and input voltage values, which are shown from Fig. 5 to Fig. 8. The power changes from 1 kW to 3 kW, and the coil parameters are the measured values, i.e., $L_1 = 338$ μH and $L_2 = 226$ μH. The mutual inductance is selected between 70 μH and 105 μH, which corresponds to a coupling coefficient between 0.25 and 0.38. For LCC-S compensation, $L_f = 100$ μH.

A. S-S Compensation

Fig. 5 and Fig. 6 show the simulated and calculated peak voltage across the primary and secondary coils when M is 70 μH and 105 μH, respectively.

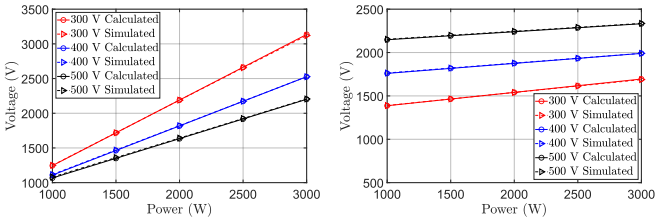

(a) (b)

Fig. 5: S-S compensation, $M = 70$ μH. (a) Peak voltage of primary coil. (b) Peak voltage of secondary coil.

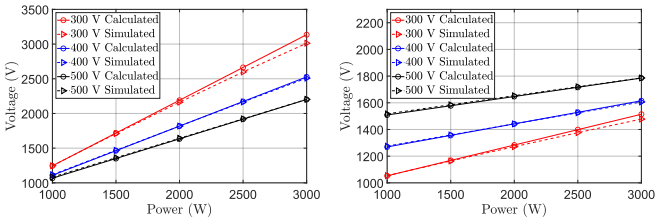

(a) (b)

Fig. 6: S-S compensation, $M = 105$ μH. (a) Peak voltage of primary coil. (b) Peak voltage of secondary coil.

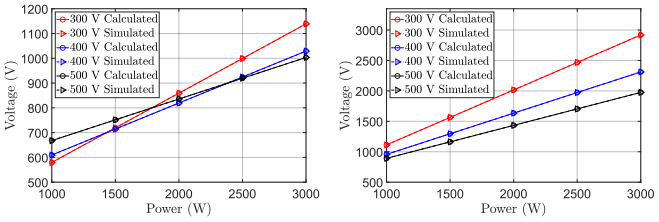

(a) (b)

Fig. 7: LCC-S compensation, $M = 70$ μH. (a) Peak voltage of L_f. (b) Peak voltage of secondary coil.

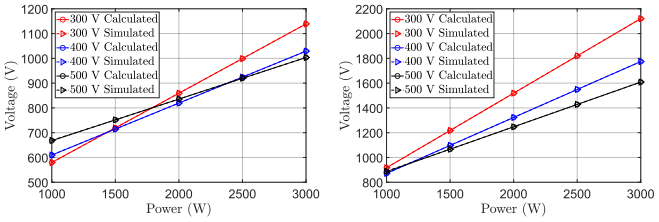

(a) (b)

Fig. 8: LCC-S compensation, $M = 105$ μH. (a) Peak voltage of L_f. (b) Peak voltage of secondary coil.

B. LCC-S Compensation

Fig. 7 and Fig. 8 show the simulated and calculated peak voltage across L_f and secondary coil when M is 70 μH and 105 μH, respectively.

It can be seen that the calculated peak voltage values match the simulation results well for both compensations. For LCC-S compensation, the two values are almost the same, so, the two lines coincide. For S-S compensation, due to the small power mismatch between simulation and calculation in some cases, the two peak voltage values could have a small difference.

V. Experimental Verification

The experiment setup with LCC-S compensation is shown in Fig. 9. For the experiment, the mutual inductance M was measured to be 105 μH at a vertical distance around 10 cm. The inductance value of L_f is 100.5 μH. Based on the voltage rating of the available differential probes of Keysight N2791A and Yokogawa 700924, the WPT prototype was tested at a lower voltage and power value.

A. S-S Compensation

Fig. 10 shows the measurement results with $V_{in} = 200$ V and $P_o = 500$ W.

Fig. 11 shows the peak voltage of the coils under different input voltage values when $P_o = 500$ W.

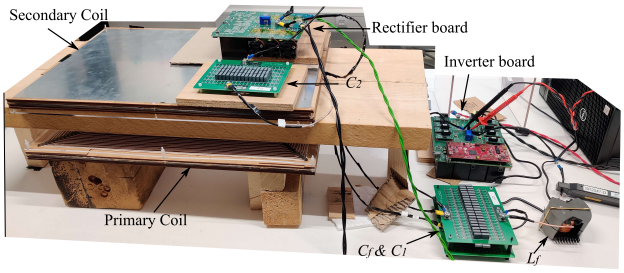

Fig. 9: Experiment setup with LCC-S compensation.

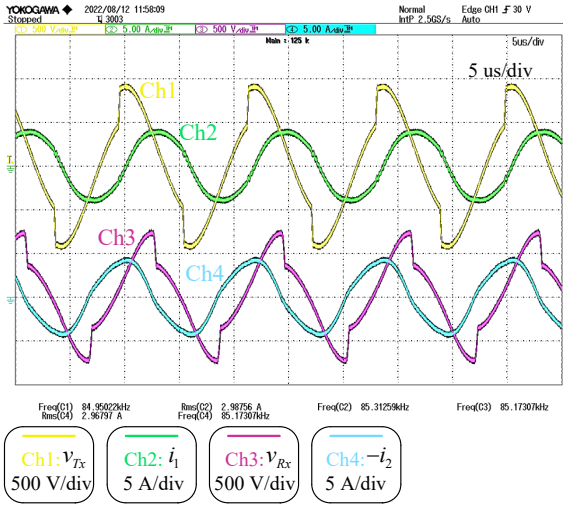

(a)

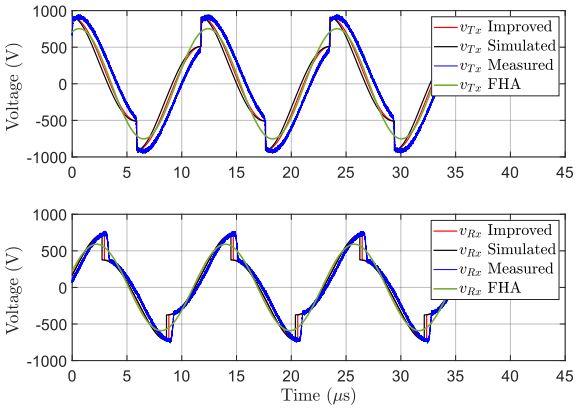

(b)

Fig. 10: Experimental results of S-S compensation operating at $V_{in} = 200$ V and $P_o = 500$ W, defined reference direction is shown in Fig. 2. (a) Measured waveforms. (b) Voltage waveforms of v_{Tx} and v_{Rx} based on improved method, simulation, measurement and FHA method.

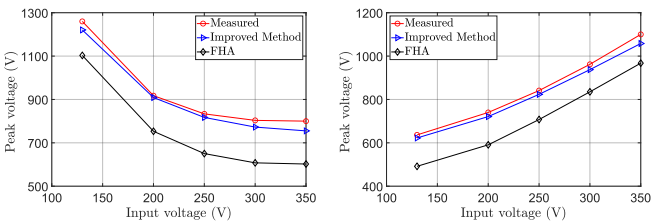

(a) (b)

Fig. 11: S-S compensation, peak voltage across coils at 500 W from measurement, improved and FHA method. (a) Peak voltage of primary coil. (b) Peak voltage of secondary coil.

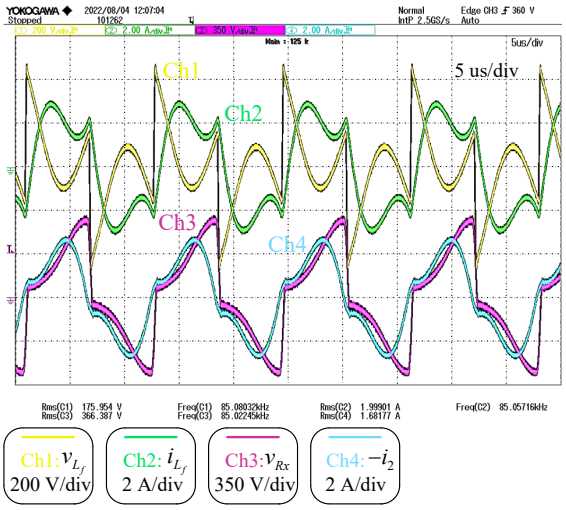

(a)

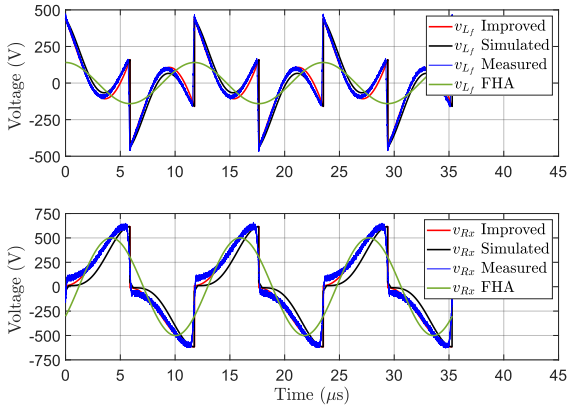

(b)

Fig. 12: Experimental results of LCC-S compensation operating at $V_{in} = 300$ V and $P_o = 500$ W, defined reference direction is shown in Fig. 2. (a) Measured waveforms. (b) Voltage waveforms of v_{L_f} and v_{Rx} based on improved method, simulation, measurement and FHA method.

B. LCC-S Compensation

Fig. 12 shows the measurement results with $V_{in} = 300$ V and $P_o = 500$ W.

Fig. 13 shows the peak voltage of L_f and secondary coil under different input voltage values when $P_o = 500$ W.

As it can be seen from the experiments, the improved

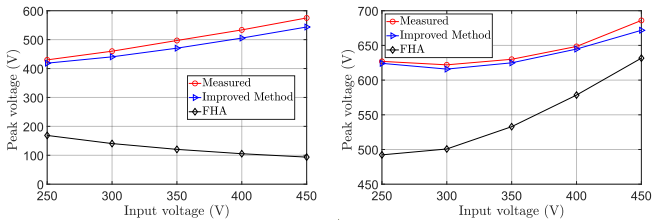

(a) (b)

Fig. 13: LCC-S compensation, peak voltage across L_f and secondary coil at 500 W from measurement, improved and FHA method. (a) Peak voltage of L_f. (b) Peak voltage of secondary coil.

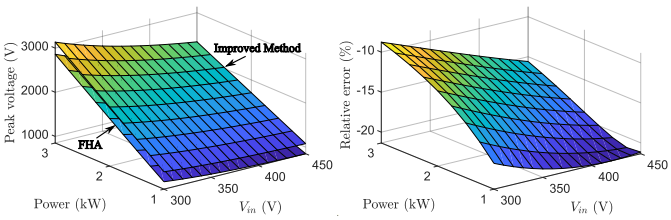

(a) (b)

Fig. 14: S-S compensation. (a) Peak voltage of primary coil. (b) Relative error.

formulas can provide accurate peak voltage results for both S-S and LCC-S compensations. The improved piecewise voltage analytic function is given in Appendix B.

It should be noted that in practical application, the resonant compensation circuit will usually be tuned to be a bit inductive for zero voltage switching (ZVS) turn-on of the front-end full-bridge inverter, which could introduce some calculation error, for example, by further checking at Fig. 10(a), it can be found that the voltage step change does not occur at the peak of the sinusoidal part. However, this error can be neglected at designed rated condition when the components bear the maximum stress.

C. Voltage Stress in a Wider Operational Range

Herein, the voltage stresses will be calculated and compared in a wider operational range based on the FHA and improved methods. The relative error between these two methods will be given with the expression of $\varepsilon = \frac{\text{Value of FHA}-\text{Value of Improved Method}}{\text{Value of Improved Method}}$.

Below, $L_1 = 338$ μH, $L_2 = 226$ μH, $M = 105$ μH, $L_f = 100$ μH.

1) S-S Compensation: The results are given in Fig. 14 and Fig. 15.

2) LCC-S Compensation: The results are given in Fig. 16 and Fig. 17.

VI. Conclusion

An improved peak voltage calculation method for compensation components is introduced in wireless power transfer systems employing S-S and LCC-S compensation topologies, which is often ignored in current literature. This method is verified by both simulation and experimental results, which provides practical guidance for the design of WPT systems, especially for electrical insulation design. The introduced method can also be applied to other compensation networks such as LCC-LCC compensation topology in a similar way. In essence,

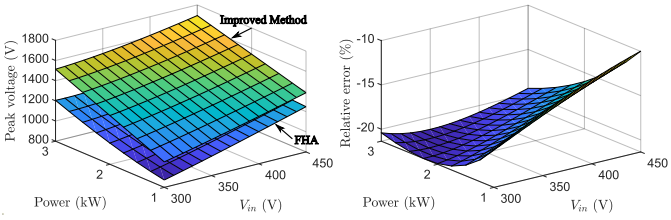

(a) (b)

Fig. 15: S-S compensation. (a) Peak voltage of secondary coil. (b) Relative error.

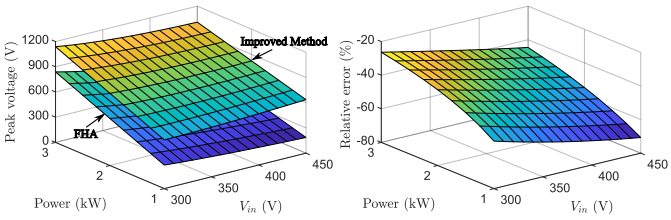

(a) (b)

Fig. 16: LCC-S compensation. (a) Peak voltage of L_f. (b) Relative error.

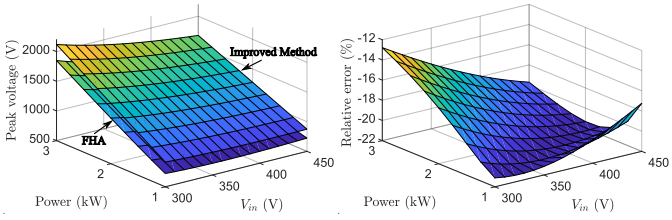

(a) (b)

Fig. 17: LCC-S compensation. (a) Peak voltage of secondary coil. (b) Relative error.

the accuracy of the introduced method depends on the related compensation capacitor voltage calculation under FHA method, which condition is often satisfied for a well-designed WPT system.

APPENDIX A

For reading convenience, the equation is re-given below

$$v_{L_f} = v_{AB} - v_{C_f}, \dot{V}_{C_f} = \dot{V}_s - jZ_r\frac{\dot{V}_s}{\omega_0 L_f}, Z_r = \frac{\omega_0^2 M^2}{R_{ac}}. \tag{17}$$

As it can be seen from (17), the phase delay of v_{C_f} relative to the fundamental frequency component of v_{AB} is less than $\frac{\pi}{2}$ radian and larger than zero (cf. Fig. 4(a), i.e., $0 < \frac{t_d}{T_0} < \frac{1}{4}$ with T_0 being the switching period), therefore, the voltage of v_{L_f} has and only has three local peaks.

The voltage across L_f at P_1, P_2 and P_3 can be calculated as

$$\begin{cases} v_{L_f\_P_1} = V_{in} + \sqrt{2}\frac{\omega_0 M^2}{L_f R_{ac}} V_s, \\ v_{L_f\_P_2} = [\sqrt{2} \times \sqrt{1 + (\frac{\omega_0 M^2}{L_f R_{ac}})^2} - \frac{\pi}{2\sqrt{2}}]V_s, \\ v_{L_f\_P_3} = V_{in} - \sqrt{2}\frac{\omega_0 M^2}{L_f R_{ac}} V_s. \end{cases} \tag{18}$$

From (18), it is clear that $v_{L_f\_P_1}$ is larger than $v_{L_f\_P_3}$. The voltage difference between P_1 and P_2 is

$$\begin{aligned} &\Delta v_{L_f\_P_1P_2} = v_{L_f\_P_1} - v_{L_f\_P_2} \\ &= \sqrt{2}V_s[\tfrac{\pi}{2} + \tfrac{\omega_0 M^2}{L_f R_{ac}} - \sqrt{1 + (\tfrac{\omega_0 M^2}{L_f R_{ac}})^2}]. \end{aligned} \tag{19}$$

Since (19) is always larger than 0, therefore, $v_{L_f\_P_1}$ is larger than $v_{L_f\_P_2}$. Summarizing, the voltage across L_f at P_1 instant is the maximum voltage in one period.

APPENDIX B

Without loss of generality, assuming the time instant when v_{AB} passes zero from $-V_{in}$ to V_{in} is 0 s, and T_0 is the switching period, then the time domain expressions are as follows:

A. S-S Compensation

$$v_{Tx}(t) = \begin{cases} V_{in} + \hat{V}_{C_1}\sin(\omega_0 t + \frac{\pi}{2}), t \in [0, \frac{T_0}{2}), \\ -V_{in} + \hat{V}_{C_1}\sin(\omega_0 t + \frac{\pi}{2}), t \in [\frac{T_0}{2}, T_0). \end{cases} \tag{20}$$

$$v_{Rx}(t) = \begin{cases} V_{out} + \hat{V}_{C_2}\sin(\omega_0 t), t \in [0, \frac{T_0}{4}), \\ -V_{out} + \hat{V}_{C_2}\sin(\omega_0 t), t \in [\frac{T_0}{4}, \frac{3T_0}{4}), \\ V_{out} + \hat{V}_{C_2}\sin(\omega_0 t), t \in [\frac{3T_0}{4}, T_0). \end{cases} \tag{21}$$

In (20) and (21), $\hat{V}_{C_1} = \dfrac{\pi\omega_0 L_1 P_o}{2V_{in}}$, $\hat{V}_{C_2} = \dfrac{4L_2 V_{in}}{\pi M}$.

B. LCC-S Compensation

$$v_{L_f}(t) = \begin{cases} V_{in} - \hat{V}_{C_f}\sin(\omega_0 t + \varphi), t \in [0, \frac{T_0}{2}), \\ -V_{in} - \hat{V}_{C_f}\sin(\omega_0 t + \varphi), t \in [\frac{T_0}{2}, T_0). \end{cases} \tag{22}$$

$$v_{Rx}(t) = \begin{cases} V_{out} + \hat{V}_{C_2}\sin(\omega_0 t - \frac{\pi}{2}), t \in [0, \frac{T_0}{2}), \\ -V_{out} + \hat{V}_{C_2}\sin(\omega_0 t - \frac{\pi}{2}), t \in [\frac{T_0}{2}, T_0). \end{cases} \tag{23}$$

In (22) and (23), $\varphi = -\arctan\dfrac{\omega_0 L_f P_o}{V_s^2}$, $\hat{V}_{C_f} = \sqrt{2}\omega_0 L_f\sqrt{(\frac{P_o}{V_s})^2 + (\frac{V_s}{\omega_0 L_f})^2}$ and $\hat{V}_{C_2} = \dfrac{\pi\omega_0 L_2 L_f P_o}{2MV_{in}}$.

REFERENCES

[1] J. Garnica, R. A. Chinga and J. Lin, "Wireless Power Transmission: From Far Field to Near Field," in Proceedings of the IEEE, vol. 101, no. 6, pp. 1321-1331, June 2013, doi: 10.1109/JPROC.2013.2251411.

[2] Y. Chen, H. Zhang, C. -S. Shin, K. -H. Seo, S. -J. Park and D. -H. Kim, "A Comparative Study of S-S and LCC-S Compensation Topology of Inductive Power Transfer Systems for EV Chargers," 2019 IEEE 10th International Symposium on Power Electronics for Distributed Generation Systems (PEDG), 2019, pp. 99-104, doi: 10.1109/PEDG.2019.8807684.

[3] F. Grazian, W. Shi, T. B. Soeiro, J. Dong, P. van Duijsen and P. Bauer, "Compensation Network for a 7.7 kW Wireless Charging System that Uses Standardized Coils," 2020 IEEE International Symposium on Circuits and Systems (ISCAS), 2020, pp. 1-5, doi: 10.1109/ISCAS45731.2020.9181016.

[4] W. Shi et al., "Design of a Highly Efficient 20-kW Inductive Power Transfer System With Improved Misalignment Performance," in IEEE Transactions on Transportation Electrification, vol. 8, no. 2, pp. 2384-2399, June 2022, doi: 10.1109/TTE.2021.3133759.

[5] F. Corti et al., "A Comprehensive Comparison of Resonant Topologies for Magnetic Wireless Power Transfer," 2020 IEEE 20th Mediterranean Electrotechnical Conference (MELECON), 2020, pp. 582-587, doi: 10.1109/MELECON48756.2020.9140657.

[6] A. Cavallini, D. Fabiani and G. C. Montanari, "Power electronics and electrical insulation systems - Part 1: Phenomenology overview," in IEEE Electrical Insulation Magazine, vol. 26, no. 3, pp. 7-15, May-June 2010, doi: 10.1109/MEI.2010.5482783.

[7] A. Cavallini, D. Fabiani and G. C. Montanari, "Power electronics and electrical insulation systems - part 2: life modeling for insulation design," in IEEE Electrical Insulation Magazine, vol. 26, no. 4, pp. 33-39, July-Aug. 2010, doi: 10.1109/MEI.2010.5511187.

[8] Wireless Power Transfer for Light-Duty Plug-in/Electric Vehicles and Alignment Methodology, SAE International, October 2020, revised.

[9] Z. Zhang, H. Pang, A. Georgiadis and C. Cecati, "Wireless Power Transfer—An Overview," in IEEE Transactions on Industrial Electronics, vol. 66, no. 2, pp. 1044-1058, Feb. 2019, doi: 10.1109/TIE.2018.2835378.

[10] R. L. Steigerwald, "A comparison of half-bridge resonant converter topologies," in IEEE Transactions on Power Electronics, vol. 3, no. 2, pp. 174-182, April 1988, doi: 10.1109/63.4347.